Low-Temperature Turnover Control of Photosystem II Using Novel Metal-Containing Redox-Active Herbicides

ARTICLE *in* JOURNAL OF THE AMERICAN CHEMICAL SOCIETY · MAY 2000

Impact Factor: 12.11 · DOI: 10.1021/ja994138x

Low-Temperature Turnover Control of Photosystem II Using Novel Metal-Containing Redox-Active Herbicides

Laba Karki, K. V. Lakshmi, Veronika A. Szalai,† and Gary W. Brudvig*

Contribution from the Department of Chemistry, Yale University, P.O. Box 208107, New Haven, Connecticut 06520-8107

Received November 29, 1999

Abstract: A novel approach of using metal-containing redox-active herbicides to prepare and study the light-induced intermediates of the photosystem II (PSII) photocycle is described. The redox-active herbicides feature an iron(III) ethylenediaminetetracetate [Fe^{III}−(EDTA)] electron-acceptor group linked to a Q_B-site binding dimethylphenylurea moiety by a hydrocarbon spacer. Like the nitroxyl-based redox-active herbicides previously described (Bocarsly, J. R.; Brudvig, G. W. *J. Am. Chem. Soc.* **1992**, *114*, 9762−9767), metal-containing herbicides accept electrons from the donor side of PSII while bound to the Q_B site and restrict the S-state cycling to two stable charge separations. The use of Fe^{III}−(EDTA) as an electron acceptor allows turnover at low temperatures. EPR studies of PSII upon continuous illumination at 225 K with 0.7 mM of redox-active herbicide, Fe^{III}−(EDTA) linked by an ethane spacer to a dimethylphenyl urea group (**4**), produced a stable two-step S_1 to S_3 advance of the O_2-evolving complex (OEC) and a stoichiometric reduction of the Fe^{III}−(EDTA) moiety of the herbicide, while a control sample with 0.02 mM DCMU [3-(3,4-dichlorophenyl)-1,1-dimethyl-urea] and 0.7 mM of **4** exhibited only a one-step S_1 to S_2 advance of the OEC without significant reduction of the Fe^{III}−(EDTA) moiety of the herbicide. Similar EPR results were obtained for **7**, Fe^{III}−(EDTA) linked to the dimethylphenylurea group by a pentane spacer. O_2-evolution inhibition studies show that appending the Fe^{III}−(EDTA) moiety to the phenylurea herbicide causes a significant decrease in the binding affinity compared to that of DCMU. On the basis of O_2-evolution studies with various herbicide derivatives and different PSII sample types, the observed decrease in binding affinities is attributed to the degree of accessibility of the Q_B-binding pocket to the herbicides and to electrostatic and hydrophilicity factors. The present study describes the use of novel metal-containing herbicides in studying long-range electron transfer in PSII and in trapping photogenerated two-electron oxidized intermediate states of the O_2-evolving complex.

Introduction

Photosystem II (PSII), a multicomponent plant membrane protein complex, harvests light energy to couple the oxidation of water to dioxygen with the concomitant reduction of plastoquinone.[1] Absorption of photons by the primary chlorophyll electron donor, P_{680}, initiates electron transfer from P_{680} through a pheophytin molecule ($Pheo_A$) to a primary quinone electron acceptor (Q_A) and finally to a reversibly bound plastoquinone (PQ) at the Q_B-binding pocket.[2] After the second photoinduced electron-transfer step, the plastoquinone becomes fully reduced to PQH_2 and leaves the binding pocket, creating a two-electron gate to electron transfer. While the plastoquinone accepts electrons from the excited P_{680}* molecule, the O_2-evolving complex (OEC), consisting of a tetranuclear manganese cluster (Mn_4), donates reducing equivalents of electrons to P_{680}^+ via a tyrosine residue called Tyr_Z (Y_z).[3] According to the Kok model,[4] the tetranuclear manganese cluster (Mn_4) accesses higher oxidation S_i states ($i = 0-4$) by successive photoinduced electron-transfer steps and releases a molecule of dioxygen in the S_4 to S_0 turnover (Scheme 1).[1,4]

Scheme 1

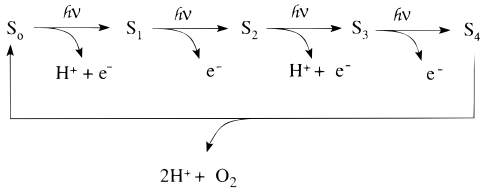

Since the elucidation of the S-state cycle, spectroscopic studies have been carried out to gain structural information on each of the S states to understand their role in the water-oxidation chemistry. However, complete characterization of the higher oxidation S_3 state has remained a challenge because of its limited stability and the difficulty in isolating this state in high yield. Although flash-induced methods[5] have produced ∼50% yield of the S_3 state in concentrated samples for spectroscopic studies, characterization by parallel mode EPR[6] and EXAFS[7] has yielded only preliminary information. Besides flash-induced methods, redox-active herbicide inhibitors such

* To whom correspondence should be addressed. Telephone: 203-432-5202. Fax: 203-432-6144. E-mail: gary.brudvig@yale.edu.

† Current address: Department of Chemistry, University of North Carolina at Chapel Hill, NC 27599-3290.

(1) Debus, R. J. *Biochim. Biophys. Acta* **1992**, *1102*, 269−352.

(2) Diner, B. A.; Babcock, G. T. In *Oxygenic Photosynthesis: The light reactions*; Ort, D. R., Yocum, C. F., Eds.; Kluwer Academic Publishers: Dordrecht, The Netherlands, 1996; Vol. 4, pp 213−247.

(3) (a) Debus, R. J.; Barry, B. A.; Sithole, I.; Babcock, G. T.; McIntosh, L. *Biochemistry* **1988**, *27*, 9071−9074. (b) Metz, J. G.; Nixon, P. J.; Rögner, M.; Brudvig, G. W.; Diner, B. A. *Biochemistry* **1989**, *28*, 6960−6969.

(4) Kok, B.; Forbush, B.; McGloin, M. *Photochem. Photobiol.* **1970**, *11*, 457−475.

(5) Styring, S.; Rutherford, A. W. *Biochemistry* **1987**, *26*, 2401−2405.

(6) Matsukawa, T.; Mino, H.; Yoneda, D.; Kawamori, A. *Biochemistry* **1999**, *38*, 4072−4077.

10.1021/ja994138x CCC: $19.00
Published on Web 05/12/2000

Scheme 2

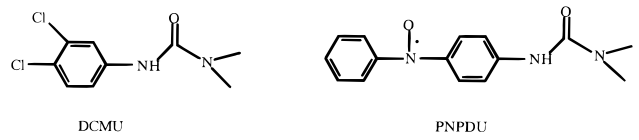

as dimethylureido phenyl phenyl nitroxide (PNPDU, Scheme 2), have also been used to generate the S_3 state in 75% yield (Scheme 3).[8] The ability of the redox-active herbicides to bind tightly to the Q_B-binding site and accept one electron from Q_A enables the formation of a two-electron charge-separated state in high yield. Although PNPDU accepts an electron in advancing the Mn_4 cluster from the S_2 to S_3 state, its applicability is limited to temperatures of ≥ 250 K owing mainly to the proton-coupling requirement for electron transfer. One approach to produce a double turnover at temperatures lower than 250 K is by using metal-containing redox-active herbicides that do not involve proton-coupling in the electron-transfer step. Herbicides that can accept electrons at lower temperatures would allow for new possibilities to trap and study photogenerated intermediate states such as the $S_2Y_z^{\bullet}$ state that has previously been studied only in inhibited samples.[9]

In light of the ongoing studies to unravel structural information about the S_3 and possibly the $S_2Y_z^{\bullet}$ states, we demonstrate the versatility of using novel metal-containing redox-active herbicides with an Fe^{III}−(EDTA) electron-acceptor group linked by a hydrocarbon spacer to a phenyldimethyl urea herbicide for studying photochemical turnover of PSII at temperatures below 250 K. Metal-based acceptors provide additional structural flexibility in studying the mechanisms, energetics and rates of long-range electron transfer to the Q_B site. The work reported herein also demonstrates the use of a covalent tether between an active-site binding moiety and a redox-active moiety for controlled transfer of electrons out of a protein active site. In a related study, Wilker et al.[10] have recently demonstrated the design and use of photosensitizers linked by hydrocarbon spacers to binding groups that have high affinity for the cytochrome $P450_{cam}$ heme pocket. By delivering holes or electrons directly to the active site, these charge-transfer complexes allowed the preparation and study of redox intermediates of cytochrome P450. We demonstrate here the use of metal complexes linked by hydrocarbon spacers to a phenyl urea herbicide with an affinity for the Q_B site to prepare and study transient states in the PSII photocycle.

Experimental Section

Materials and Instruments. All reagent grade chemicals and solvents were purchased from commercial vendors. Iron(III) nitrate [$Fe(NO_3)_3{\cdot}9H_2O$], BOC−ON [2-(*tert*-butoxycarbonyloxyimino)-2-phenylaceto-nitrile] and ethylenediamine were purchased from Aldrich and used as received. Other chemicals including mono-*tert*-butoxycarbonyl 1,5-diaminopentane toluenesulfonic acid salt (Nova BioChem), *N*,*N*′-dicyclohexylcarbodiimide (DCC, Acros Organics) and *N*-hydroxysuccinimide (NHS, Pierce Chemical Co.) were also used as received. *n*-dodecyl-*β*-D-maltoside was purchased from Anatrace and used as received. Thin-layer chromatography (TLC) was performed on polymer backed silica gel plates (60 Å, Aldrich). Column chromatography was performed on silica gel 200−400 mesh (60 Å, Aldrich). High performance liquid chromatography (HPLC) was performed with a computer-controlled system (Rainin, model Dynamax SD-200) with a diode array detector on a Vydac C-18 (1 cm × 25 cm) reverse phase column. Visible spectra were measured on a Perkin-Elmer Lambda 3B spectrophotometer. NMR spectra were recorded on an Oxford QE-Plus 300 MHz spectrometer.

Synthesis of BOC-Protected Ethylenediamine, BOC-EN[11] (1). To a warm (45 °C) solution of ethylenediamine (34 mL, 0.51 mol) in 60 mL of THF, BOC-ON (25.0 g, 0.102 mol) in 80 mL of THF was added dropwise continuously. The solution was stirred for 20 min, and a yellow product was recovered after removing excess ethylenediamine and THF in vacuo. Yield: 70%. ^{1}H NMR in $CDCl_3$ (ppm): δ 1.4 (9 H, s, BOC group); δ 3.0 (2 H, m, CH_2); δ 3.2 (2 H, m, CH_2); δ 4.0 (2 H, broad, NH_2); δ 5.0 (1 H, t, N−H). Impurities due to the phenyl groups of the BOC−ON were observed at δ 7.4 (2 H, m, aromatic); δ 7.8 (2 H, m, aromatic).

Synthesis of BOC-EN-SO_2R (2).[11,12] To a solution of 1,1-dimethyl-3-[4-(chlorosulfonyl)phenyl]urea [**RSO_2Cl**][8] (4.0 g, (15 mmol) in 150 mL of THF), 2.43 g (15 mmol) of **1** in 100 mL of THF was added dropwise over 1 h with continuous stirring. After adding 20 mL of water to this mixture, the solution was refluxed at 60−70 °C. After 2 h, the solution was allowed to cool to room temperature. The organic layer was separated and washed with 2 × 5 mL portions of saturated sodium bicarbonate ($NaHCO_3$) followed by 2 × 5 mL portions of saturated NaCl solution. The organic layer was dried over anhydrous $MgSO_4$, filtered, and concentrated under reduced pressure affording a yellowish, sticky product. Performance of TLC with a solvent mixture of (5:5:1) ethyl acetate:hexane:methanol resulted in three bands. The slowest moving band was deduced to be the coupled product from a comparison with the R_f values of the starting materials. Purification was accomplished with silica gel column chromatography using a (4 × 30 cm) column, and eluting with (5:5:1) ethyl acetate:hexane:methanol solvent mixture. The BOC-protected product eluted as the final band. Yield: ∼60%. TLC: $R_f = 0.23$ on SiO_2 with hexane:ethyl acetate:methanol (5:5:1). ^{1}H NMR in $(CD_3)_2O$ (ppm): δ 1.4 (9 H, s, BOC group); δ 2.9 (2 H, m, ethyl); δ 3.2 (2 H, m, ethyl); δ 3.0 (6 H, s, $N(CH_3)_2$); δ 6.1 (1 H, s, N−H); δ 6.4 (1 H, t, N−H); δ 7.8 (4 H, q, aromatic); δ 8.2 (1 H, s, N−H). Anal. Calcd. for $C_{16}H_{26}N_4O_5S_1$: C, 49.7; H, 6.78; N, 14.5. Found: C, 48.5; H, 6.42; N, 14.1.

Deprotection of the BOC Group, NH_2-EN-SO_2R (3). 0.5 g of **2** was dissolved in 5 mL TFA/30 mL CH_2Cl_2 and stirred under nitrogen for several hrs. The solvent was removed under reduced pressure affording a yellow sticky residue that was recrystallized from methanol/ether solution yielding a white microcrystalline product. Yield: ∼90%. ^{1}H NMR in $(CD_3)_2O$ (ppm): δ 2.5 (2 H, d, NH_2); δ 3.0 (6 H, s, $N(CH_3)_2$); δ 3.25 (2 H, m, ethyl); δ 3.9 (2 H, m, ethyl); δ 7.7 (4 H, s, aromatic); δ 7.9 (1 H, t, N−H); δ 8.2 (1 H, s, N−H). Anal. Calcd. for $C_{11}H_{18}N_4O_3S_1$: C, 46.13; H, 6.33; N,19.57. Found: C, 45.26; H, 6.44; N, 19.04.

Synthesis of Fe^{III}−(EDTA)-EN-SO_2R (4)[12] (Figure 1). 400 mg (105.6 mmol) of Fe^{III}−(EDTA)·$2H_2O$[13] was dissolved in 10 mL of anhydrous DMF and stirred at 0 °C under a dry nitrogen atmosphere. After the solution turned clear, 0.216 g (105.6 mmol) of DCC and 0.060 g (105.6 mmol) of NHS were added and stirred. After 10 min, 0.15 g (52.8 mmol) of **3** was added followed by a few drops of triethylamine (base) while the reaction mixture was allowed to warm to room

(7) Guiles, R. D.; Zimmerman, J.-L.; McDermott, A.; Yachandra, V. K.; Cole, J. L.; Dexheimer, S. L.; Britt, R. D.; Wieghardt, K.; Bossek, U.; Sauer, K.; Klein, M. P. *Biochemistry* **1990**, *29*, 471−475.

(8) Bocarsly, J. R.; Brudvig, G. W. *J. Am. Chem. Soc.* **1992**, *114*, 9762−9767.

(9) (a) Szalai, V. A.; Kühne, H.; Lakshmi, K. V.; Brudvig, G. W. *Biochemistry* **1998**, *37*, 13594−13603. (b) Tang, X.-S.; Randall, D. W.; Force, D. A.; Diner, B. A.; Britt, R. D. *J. Am. Chem. Soc.* **1996**, *118*, 7638−7639. (c) Szalai, V. A.; Brudvig, G. A. *Biochemistry* **1996**, *35*, 1946−1953. (d) Boussac, A.; Rutherford, A. W. *Biochemistry* **1988**, *27*, 3476−3483. (e) MacLachlan, D. J.; Nugent, J. H. A. *Biochemistry* **1993**, *32*, 9772−9780. (f) Lakshmi, K. V.; Eaton, S. S.; Eaton, G. R.; Frank, H. A.; Brudvig, G. A. *J. Phys. Chem. B* **1998**, *102*, 8327−8335.

(10) Wilker, J. J.; Dmochowski, I. J.; Dawson, J. H.; Winkler, J. R.; Gray, H. B. *Angew. Chem., Int. Ed.* **1999**, *38*, 90−92.

(11) Reifler, M. J. Ph.D. Thesis, Yale University, New Haven, 1998.

(12) Ermacora, R. M.; Delfino, J. M.; Cuenoud, B.; Schepartz, A.; Fox, R. O. *Proc. Natl. Acad. Sci. U.S.A.* **1992**, *89*, 6383−6387. (b) Hertzberg, R. P.; Dervan, P. *J. Am. Chem. Soc.* **1982**, *104*, 313−315. (c) Sluka, J. P.; Griffin, J. H.; Mack, D. P.; Dervan, P. B. *J. Am. Chem. Soc.* **1990**, *112*, 6369−6374. (d) Ebright, Y. W.; Chen, Y.; Pendergrast, S. P.; Ebright, R. H. *Biochemistry* **1992**, *31*, 10664−10670.

(13) Basallote, M. G.; Alcala, J. M. L.; Vizcaino, M. C. P.; Vilchez, F. G. *Inorg. Synth.* **1986**, *24*, 207−208. (b) Hoard, J. L.; Kennard, C. H. L.; Smith, G. S. *Inorg. Chem.* **1963**, *2*, 1316−1317.

Scheme 3

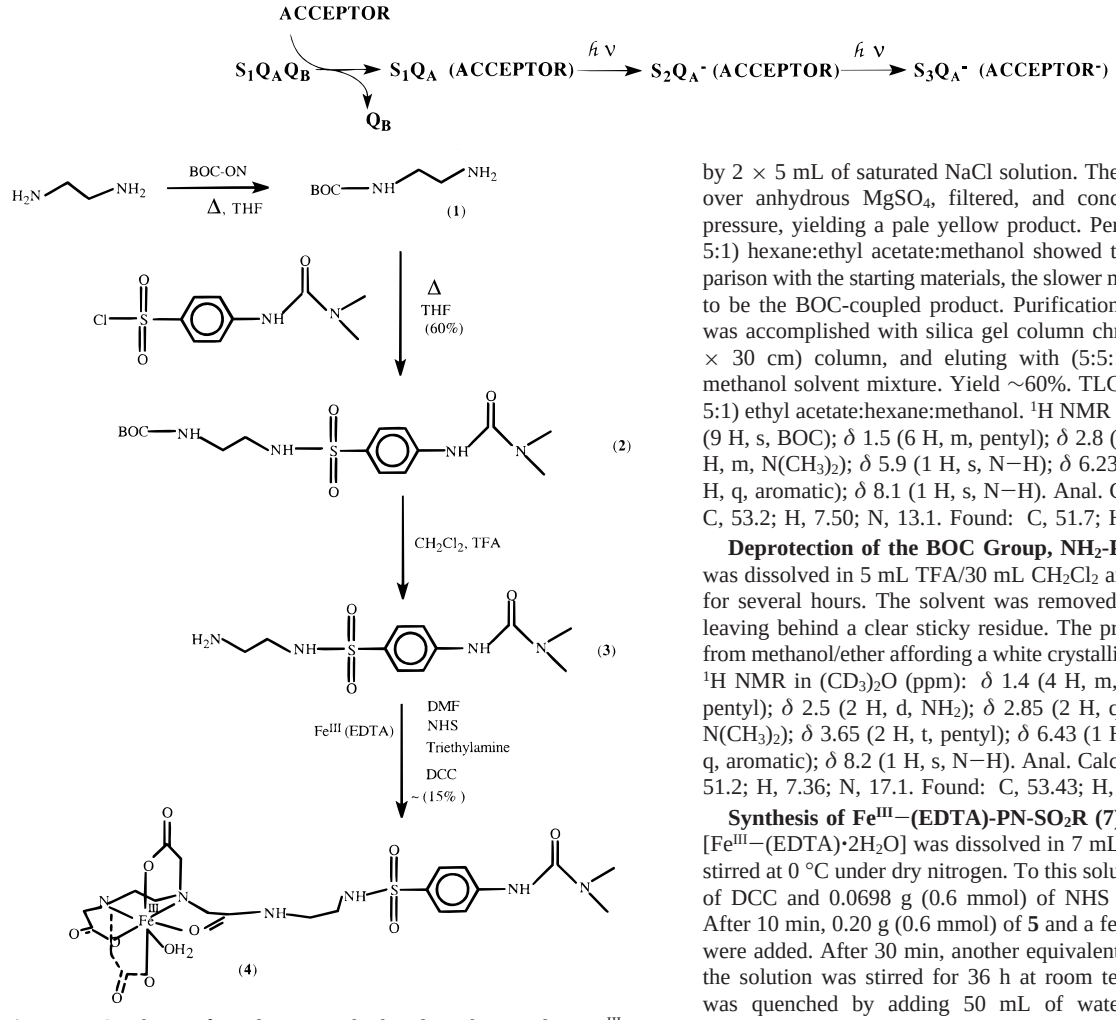

Figure 1. Synthesis of a redox-active herbicide, **4**, by coupling Fe^{III}−(EDTA) to a primary amine group of a hydrocarbon spacer using *N*,*N*′-dicyclohexylcarbodiimide (DCC).

temperature. After 30 min, 0.108 g (52.8 mmol) of DCC was added to the reaction mixture to compensate for any loss of DCC due to hydrolysis. After 36 h, the reaction was quenched by adding excess (∼50 mL) of water. The resulting white precipitate, dicyclohexyl urea (DCU), was isolated by filtration. The yellow filtrate was concentrated under reduced pressure leaving the product in neat DMF (2−3 mL). Neat toluene was then added dropwise, resulting in a yellow precipitate. Finally, this yellow solid was isolated by filtration, washed with toluene, acetone, and diethyl ether, and stored in a desiccator. Purification of the coupled product was accomplished by using HPLC and eluting the product with two different solvent mixtures: solvent A: 98% water, 2% acetonitrile, 0.06% TFA; solvent B: 80% acetonitrile, 20% water, 0.05% TFA. The HPLC solvent gradient went from 100% A, 0% B to 80% A, 20% B in 40 min. Uncoupled Fe^{III}−(EDTA) eluted at 4 min followed by the coupled product **4** at 21 min and **3** at 24 min. Yield: ∼15%. The UV−vis spectrum of **4** showed two bands: 250 nm ($\epsilon \approx$ 26000 cm^{-1} M^{-1}) ($\pi-\pi^*$); 350 nm shoulder ($\epsilon \approx$ 5000 cm^{-1} M^{-1}) (LMCT). The compound was crystallized from water/acetone solution (see below). Anal. Calcd. for $C_{21}H_{29}N_6O_{11}S_1Fe_1$: C, 40.0; H, 4.61; N, 13.4. Found: C 39.3; H, 4.94; N, 12.9.

Synthesis of BOC-PN-SO_2R (5). To 0.5 g (1.90×10^{-3} mol) of **RSO_2Cl** in 30 mL of anhydrous THF, mono-*tert*-butoxycarbonyl 1,5-diaminopentane toluenesulfonic acid salt (BOC−PN) 0.855 g (1.2 equiv) in 60 mL of anhydrous THF was added dropwise over 1 h. After the mixture stirred for 15 min, 10 mL of water was added into the reaction mixture, and it was gently refluxed at 60 °C. After 2 more hrs, the solution was cooled to room temperature, and the organic layer was separated, washed with 2 × 10 mL of saturated $NaHCO_3$ followed by 2 × 5 mL of saturated NaCl solution. The organic layer was dried over anhydrous $MgSO_4$, filtered, and concentrated under reduced pressure, yielding a pale yellow product. Performance of TLC in (5:5:1) hexane:ethyl acetate:methanol showed two bands. From a comparison with the starting materials, the slower moving band was deduced to be the BOC-coupled product. Purification of the coupled product was accomplished with silica gel column chromatography using a (4 × 30 cm) column, and eluting with (5:5:1) ethyl acetate:hexane:methanol solvent mixture. Yield ∼60%. TLC: $R_f = 0.27$ on SiO_2 (5:5:1) ethyl acetate:hexane:methanol. ^{1}H NMR in $(CD_3)_2O$ (ppm): δ 1.4 (9 H, s, BOC); δ 1.5 (6 H, m, pentyl); δ 2.8 (4 H, m, pentyl); δ 3.0 (6 H, m, $N(CH_3)_2$); δ 5.9 (1 H, s, N−H); δ 6.23 (1 H, t, N−H); δ 7.7 (4 H, q, aromatic); δ 8.1 (1 H, s, N−H). Anal. Calcd. for $C_{19}H_{32}N_4O_5S_1$: C, 53.2; H, 7.50; N, 13.1. Found: C, 51.7; H, 7.03; N, 12.8.

Deprotection of the BOC Group, NH_2-PN-SO_2R (6). 0.5 g of **5** was dissolved in 5 mL TFA/30 mL CH_2Cl_2 and stirred under nitrogen for several hours. The solvent was removed under reduced pressure leaving behind a clear sticky residue. The product was recrystallized from methanol/ether affording a white crystalline product. Yield ∼90%. ^{1}H NMR in $(CD_3)_2O$ (ppm): δ 1.4 (4 H, m, pentyl); δ 1.5 (2 H, m, pentyl); δ 2.5 (2 H, d, NH_2); δ 2.85 (2 H, q, pentyl); δ 3.1 (6 H, s, $N(CH_3)_2$); δ 3.65 (2 H, t, pentyl); δ 6.43 (1 H, t, N−H); δ 7.65 (4 H, q, aromatic); δ 8.2 (1 H, s, N−H). Anal. Calcd. for $C_{14}H_{24}N_4O_3S_1$: C, 51.2; H, 7.36; N, 17.1. Found: C, 53.43; H, 7.58; N, 17.94.

Synthesis of Fe^{III}−(EDTA)-PN-SO_2R (7). 0.459 g (1.2 mmol) of [Fe^{III}−(EDTA)·$2H_2O$] was dissolved in 7 mL of anhydrous DMF and stirred at 0 °C under dry nitrogen. To this solution, 0.250 g (1.2 mmol) of DCC and 0.0698 g (0.6 mmol) of NHS were added and stirred. After 10 min, 0.20 g (0.6 mmol) of **5** and a few drops of triethylamine were added. After 30 min, another equivalent of DCC was added and the solution was stirred for 36 h at room temperature. The reaction was quenched by adding 50 mL of water. A white precipitate, dicyclohexylurea (DCU), was isolated by filtration. The clear yellow filtrate was concentrated under reduced pressure leaving the product in neat DMF (2−3 mL). Neat toluene was added to the DMF solution resulting in a yellow precipitate. This precipitate was isolated by filtration, washed with toluene, acetone, and diethyl ether, and dried in a desiccator. The Fe^{III}−(EDTA)-coupled herbicide was purified by running a HPLC column similar to that described for **4**. The coupled product **7** eluted at 25 min followed by **6** at 28 min. Yield: ∼15%. Anal. Calcd. for $C_{24}H_{35}N_6O_{11}S_1Fe_1$: C, 42.9; H, 5.25; N, 12.5. Found: C, 42.6; H, 5.71; N, 12.3.

Crystal Structure of 4. Single crystals of **4** were obtained by slow vapor diffusion of acetone into a saturated solution of **4** in water. Crystallographic data, intensity collection information and structural refinement parameters are provided in Table 1. All measurements were made on a Nonius Kappa CCD diffractometer with graphite monochromated Mo Kα radiation. The data were collected at −90 °C to a maximum 2θ value of 61.0°. One ϕ scan consisting of 183 data frames and omega scans consisting of 43 data frames were collected with a scan width of 1° and a detector to crystal distance, *Dx*, of 33 mm. Each frame was exposed twice (for the purpose of de-zingering) for 180 s. The data frames were processed and scaled using the DENZO software package.[14] Of the 9547 reflections collected, 7523 were unique ($R_{int} = 0.043$). No decay corrections were applied, but intensity data were corrected for SORTAV absorption[15] (absorption coefficient μ = 6.4 cm^{-1} for Mo Kα radiation) and for Lorentz and polarization effects.

The crystal structure was solved by the heavy atom Patterson method[16] and expanded using Fourier techniques.[17] The non-hydrogen

(14) Otwinowski, Z.; Minor, W. *Methods in Enzymology* **1997**, *276*, 307−326.

(15) Blessing, R. H. *Acta Cryst.* **1995**, *A51*, 33−38. (b) Blessing, R. H. *J. Appl. Cryst.* **1997**, 30, 421−426.

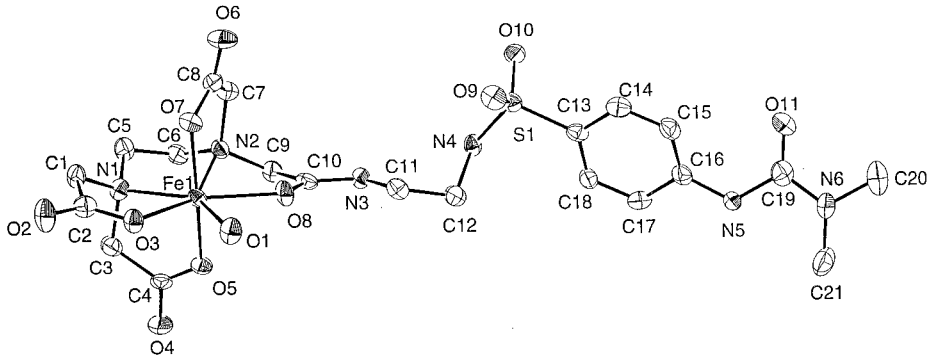

Figure 2. ORTEP view of Fe^{III}−(EDTA)−EN-SO_2R (**4**). Hydrogen atoms have been omitted for clarity. See Table 2 for the structure of R.

Table 1: Crystal Data for **4**

empirical formula	$C_{21}H_{29}N_6O_{13}SFe$
formula weight	661.40
crystal color, habit	red, plate
crystal dimensions	0.07 mm × 0.10 mm × 0.14 mm
crystal system	triclinic
lattice type	primitive
lattice parameters	
	$a = 9.096(1)$ Å
	$b = 11.389(1)$ Å
	$c = 15.700(1)$ Å
	$\alpha = 70.752(3)°$
	$\beta = 79.524(4)°$
	$\gamma = 86.918(3)°$
	$V = 1509.8(2)$ Å^3
space group	P_{-1} (#2)
Z value	2
D_{calc}	1.455 g/cm^3
F_{000}	686.00
μ (Mo Kα)	6.38 cm^{-1}
residuals: R; R_w	0.058; 0.083
goodness of fit indicator	2.12
maximum peak in final diff. map	1.24 e$^-$/Å^3
minimum peak in final diff. map	−0.36 e$^-$/Å^3

$R = \sum||F_o| - |F_c||/\sum|F_o|$; $R_w = [(\sum w(|F_o| - |F_c|)^2/\sum wF_o^2)]^{1/2}$.

atoms were refined anisotropically and hydrogen atoms were included but not refined. In the case of methyl group hydrogen atoms, one hydrogen was located in the difference map and included at an idealized distance to set the orientation of the other two hydrogen atoms. The hydrogen atoms were not observed and included for the four partial occupancy water molecules in the lattice. The final cycle of full matrix least squares refinement was based on 2906 observed reflections ($I > 5.00\ \sigma(I)$ and 397 variable parameters. The X-ray structure of **4** is shown in Figure 2.

O_2-Evolution Assays. O_2-evolution assays for the determination of the inhibition of PSII by the metal-containing redox-active herbicides were performed using a YSI Clark-type electrode. Light from a 1200 W xenon lamp (Oriel), filtered through a 10 cm water filter, a heat absorbing filter (Schott KG-5) and a long pass filter (Oriel LP 610), was directed by a Pyrex light-pipe[18] to a water-jacketed aluminum chamber maintained at 25 °C by a Neslab RTE-9DD circulator bath. Typically, 10 μg of chlorophyll spinach PSII was added in the dark into a 2.5 mL buffer solution containing 20 mM MES/NaOH (pH 6.0), 10 mM NaCl, 1 mM $K_3Fe^{III}(CN)_6$ and 250 μM 2,5-dichloro-*p*-benzoquinone (DCBQ). The O_2-evolution activity of *Synechocystis* PSII core complexes was measured in the same cell except that the buffer contained 50 mM MES/KOH, pH 6.5, 10 mM NaCl, 20 mM $CaCl_2$, 0.03% (w/v) *n*-dodecyl-β-D-maltoside, 1 mM $K_3Fe^{III}(CN)_6$, 250 μM DCBQ and 1 M sucrose. Generally, O_2-evolution activity for a given concentration of the herbicides was determined from an average of three runs. Typically, O_2-evolution activities of 375 and 3000 μmol O_2 h^{-1} (mg chlorophyll)$^{-1}$ were found for spinach and *Synechocystis* PSII samples, respectively.

Electrochemical Measurements. Electrochemical measurements were performed on an EG&G Princeton Applied Research, (model 273), potentiostat using aqueous solutions with 0.2 mM KCl supporting electrolyte. Cyclic voltammograms were recorded with a platinum disk as a working electrode, a platinum wire as a counter electrode referenced to a standard calomel electrode (SCE). Cyclic voltammograms (CV) showed reversible couples at −0.05 V vs SCE (0.2 V vs NHE) with a peak-to-peak separation of 0.07 V for [Fe^{III}−(EDTA·2H_2O] and both Fe^{III}−(EDTA)-coupled herbicides **4** and **7**.

Electron Paramagnetic Resonance (EPR) Spectroscopy. EPR measurements were performed on a Varian E-9 spectrometer equipped with a TE_{102} cavity and a helium flow cryostat (Oxford Instruments), and interfaced with a Macintosh IIci computer. Spectra of the Fe^{III}−(EDTA) moiety in the redox-active herbicides and the S_2-state of PSII were obtained under the following instrumental conditions: microwave frequency, 9.28 GHz; magnetic field modulation frequency, 100 kHz; magnetic field modulation amplitude, 20 G; scan width, 4000 G; temperature, 10 K. Due to the different concentrations of the Fe^{III}−(EDTA)-containing herbicides and the Mn_4 cluster in PSII, 0.1 mW power was applied in acquiring spectra of the Fe^{III}−(EDTA) species, while 5 mW power was applied in acquiring the S_2-multiline signals. Metmyoglobin (Sigma) was added to the EPR samples of PSII as an internal standard to quantitate the signal from the Fe^{III}−(EDTA) moiety. The EPR signal intensities of metmyoglobin ($g = 6$) and Fe^{III}−(EDTA) ($g = 4.3$) were measured from the peak-to-trough heights. The intensity of the S_2-multiline EPR signal ($g \approx 2$) was estimated as the sum of the heights of four hyperfine peak heights in the light-minus-dark difference spectra. Each spectrum was an average of 2 to 4 scans. Power saturation experiments for Fe^{III}−(EDTA)-coupled herbicide and myoglobin show no saturation effects up to 5 mW of applied microwave power at 10 K.

Photosystem II Sample Preparation. PSII membranes were isolated from market spinach leaves by a modified version[19] of the method of Berthold et al.[20] except that the thylakoid membranes were not frozen at 77 K prior to isolating the PSII membranes. Histidine-tagged (His-tag) PSII core complexes were isolated from *Synechocystis* PCC 6803 according to the method of Reifler et al.[21] After extraction, the spinach PSII membranes were suspended in buffer containing 20 mM MES/NaOH, pH 6.0, 15 mM NaCl, 30% (v/v) ethylene glycol:water and stored at 77 K. Typically, PSII samples with [chlorophyll] ([Chl]) = 8−9 mg of chlorophyll/ml (determined according to the method of

(16) Beurskens, P. T.; Admiraal, G.; Beurskens, G.; Bosman, W. P.; Garcia-Granda, S.; Gould, R. O.; Smits, J. M. M.; Smykalla, C. *PATTY*; the DIRDIF program system, Technical Report of the Crystallography Laboratory, University of Nijmegen: The Netherlands, 1992.

(17) Beurskens, P. T.; Admiraal, G.; Beurskens, G.; Bosman, W. P.; deGelder, R.; Israel, R.; Smits, J. M. M. *DIRDIF94*; the DIRDIF program system, Technical Report of the Crystallography Laboratory, University of Nijmegen: The Netherlands, 1994.

(18) Schweitzer, R.; Brudvig, G. W. *Biochemistry* **1997**, *36*, 11351−11359.

(19) Beck, W. F.; dePaula, J. C.; Brudvig, G. W. *Biochemistry* **1985**, *24*, 3035−3043.

(20) Berthold, D. A.; Babcock, G. T.; Yocum, C. F. *FEBS Lett.* **1981**, *134*, 231−234.

(21) Reifler, M. J.; Chisholm, D. A.; Wang, J.; Diner, B. A.; Brudvig, G. W. In *Photosynthesis: Mechanisms and Effects*; Garab, G., Ed.; Kluwer Academic Publishers: Dordrecht, The Netherlands, 1998; Vol. 2, pp 1189−1192.

Arnon[22]), were treated with $K_3Fe^{III}(CN)_6$ (1 mM final concentration) and incubated in the dark at 0 °C to oxidize fully cytochrome b_{559} (Cyt b_{559}). Excess ferricyanide was removed by pelleting and resuspending the PSII membranes in buffer with 20 mM MES/NaOH (pH 6.0) and 50% (v/v) ethylene glycol:water. For EPR studies, 200 μL of PSII membranes were transferred to a 4 mm (OD) quartz EPR tube (Wilmad glass) and were further treated with 50 μM ferricyanide. Herbicides **4** and **7** with the Fe^{III}−(EDTA) acceptor were added to the sample in the dark to a final herbicide concentration of 700 μM (~12-fold excess in comparison to the PSII concentration). The sample was then incubated at 0 °C for 0.5 h to allow for equilibration and diffusion of the herbicide into the Q_B-binding pocket. To this sample, 500 μM myoglobin in a buffer containing 20 mM MES/NaOH (pH 6.0) and 50% (v/v) ethylene glycol:water was added as an internal spin standard before rapidly freezing the EPR sample to 77 K. Myoglobin was chosen as an internal spin standard as it does not chemically interfere with the PSII samples and has a narrow EPR signal at $g = 6.0$ that does not overlap with the Fe^{III}−(EDTA) signal ($g = 4.3$) and the PSII signals of interest in this study.

Illumination Protocol for Turnover Experiments. EPR tubes containing the treated PSII samples were illuminated in a home-built nitrogen-flow cryostat. Prior to each illumination, the sample was incubated at the required temperature for 2−3 min to allow sufficient time for thermal equilibration. Continuous illumination (500 W/m^2) was provided by a halogen lamp. The PSII samples were first illuminated at 195 K for 3.5 min to induce the S_2 state. The S_2 to S_3 turnover was monitored by recording EPR intensity changes at 10 K following continuous illumination for varying time intervals at a given temperature (195−245 K) in the presence of the different redox-active herbicides.

Results

Strategies for Designing Metal-Containing Redox-Active Herbicides. There are basically four requirements for designing efficient redox-active herbicides. First, the herbicide should have a high affinity for the Q_B-binding pocket as evidenced by a high pI_{50} value[23] (typically pI_{50} > 3.0). Second, the herbicide should accept an electron from Q_A^- without protonation in order to enable fast and/or low-temperature turnover. Third, the acceptor's reduction potential must be higher than that of Q_A for it to accept an electron from Q_A^-. And finally, the herbicide should possess a spectroscopic handle that would enable observation and quantification of the electron-transfer reaction. Conceptually, a metal-containing herbicide featuring an Fe^{III}−(EDTA) electron-acceptor moiety linked via a hydrocarbon spacer to a Q_B-site binding functionality (dimethylphenylurea) meets all of these requirements (Figure 1). These herbicides share the same dimethylphenylurea binding group as PNPDU (Scheme 2), except that the electron-acceptor group is an Fe^{III}−(EDTA) complex. The reduction potential of **4**, 0.2 V vs NHE, is higher than that of Q_A (−0.10 V vs NHE), and electron-transfer proceeds without protonation. Furthermore, M^{III}-(EDTA) complexes (where M = Co, Ni, Fe, Cu) are seven coordinate[24] with one protonated EDTA arm available for covalent linkages via an amide bond to the dimethylphenylurea moiety. The synthesis of **4** is shown in Figure 1 where one carboxylic acid group of Fe^{III}−(EDTA) is coupled to the primary amine group of **3** using DCC as a coupling agent. It is evident from Figure 1 that varying the hydrocarbon spacer would allow for addressing the binding efficiency as well as the distance dependence of electron transfer to the Fe^{III}−(EDTA) acceptor. In addition, the paramagnetic Fe^{III} ion in these herbicides has an EPR signal in the oxidized form that is eliminated upon reduction. This EPR signature allows measurement of the extent and rate of electron transfer.

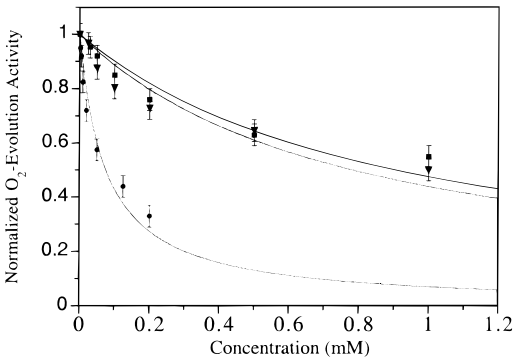

Figure 3. O_2-evolution activities as a function of concentration of **2** (●), **3** (■) and **4** (▲) at pH 6.0. The BOC-protected herbicide derivative shows one order of magnitude higher inhibition than either the free amine herbicide derivative, **3**, or the herbicide with an Fe^{III}−(EDTA) group, **4**. The error bars reflect 8% uncertainty in the measurements. The lines are least-squares fits of eq 1.

Table 2: Inhibition of O_2-Evolution from Spinach PSII Membranes by Various Herbicide Derivatives

R =

herbicide derivative	pI_{50}
DCMU	6.5
BOC-EN-SO_2R (**2**)	4.3
BOC-PN-SO_2R (**5**)	4.8
amino-EN-SO_2R (**3**)	3.4
amino-PN-SO_2R (**6**)	5.1
Fe^{III}−(EDTA)−EN-SO_2R (**4**)	3.4
Fe^{III}−(EDTA)−PN-SO_2R (**7**)	3.9

O_2-Evolution Inhibition Studies. Experiments to monitor inhibition of O_2-evolution activity were performed in the presence of the electron acceptor DCBQ (250 μM) with 1 mM ferricyanide to ensure complete oxidation of the DCBQ pool. The inhibition rates were measured for a series of nonredox-active herbicide derivatives as well as the Fe^{III}−(EDTA)-coupled herbicides. The observed O_2-evolution rates in the presence of the herbicides were modeled by eq 1:

$$v = \frac{v_{max}}{(K_I[I] + 1)} \quad (1)$$

where v is the observed rate of O_2 evolution, v_{max} is the normalized rate of O_2-evolution in the absence of an inhibitor, K_I is the equilibrium association constant between the Q_B-binding pocket and the herbicide and [I] is the inhibitor concentration. Figure 3 shows the plot of inhibition of O_2 rates by **2**, **3**, and **4**. The corresponding pI_{50} values are shown in Table 2. From Figure 3, it is evident that **2**, for which the amino group is protected, shows one order of magnitude higher inhibition of O_2-evolution rates compared to the herbicides **3** and **4**. Unlike **2** where the BOC group protects the primary amine, the BOC-deprotected primary amine, **3**, is charged in the O_2-evolution assay buffer (pH 6.0). Thus, the charged amine group of **3** and the hydrophilic Fe^{III}−(EDTA) group of **4** interact unfavorably with the polypeptide residues within the Q_B-binding pocket

(22) Arnon, D. I. *Plant Physiol.* **1949**, *24*, 1−15.

(23) The inhibitory potency of a herbicide is expressed by the equation pI_{50} = −log [I]$_{50}$ where I_{50} is the concentration at which the O_2-evolution activity is half the initial value.

(24) Zubkowski, J. D.; Perry, D. L.; Valente, E. J.; Lott, S. *Inorg. Chem.* **1995**, *34*, 6409−6411.

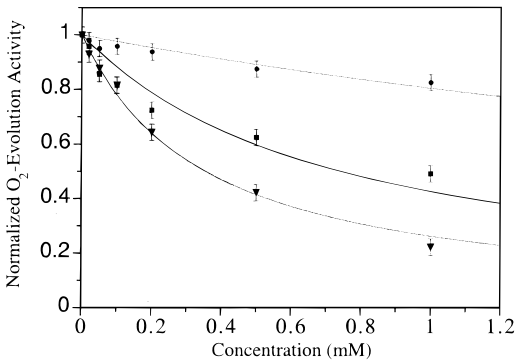

Figure 4. O_2-evolution activity as a function of concentration of **4** in different sample types: spinach thylakoid membranes (●), spinach PSII membranes (■), *Synechocystis* PSII core complexes (▲). The error bars reflect 8% uncertainty in the measurements. The lines are least-squares fits of eq 1.

leading to a substantial loss in binding affinity.[11,25] Moreover, the different pI_{50} values for the series of herbicide derivatives shown in Table 2 indicate that addition of functionalized groups beyond the DCMU parent structure leads to less efficient binding to the Q_B site.[26] Nevertheless, adding hydrocarbon spacers via a sulfonamide bond at the para-position of the phenylurea moiety of the DCMU structure results in acceptable binding and good inhibition. Furthermore, adding a longer hydrocarbon spacer between the phenylurea moiety and the Fe^{III}−(EDTA) group leads to tighter binding as evidenced by the increase in the pI_{50} values for the pentane spacer herbicide derivatives compared to those for the ethane spacer herbicide derivatives.[27] One likely explanation for the increased binding affinity with the pentane spacer is the removal of the charged amine and hydrophilic Fe^{III}−(EDTA) groups farther away from the hydrophobic residues in the Q_B-binding site, leading to less unfavorable electrostatic interactions.

To address the ability of the metal-containing herbicides to access the Q_B-binding pocket in PSII, rates of O_2-evolution inhibition were compared for thylakoid and PSII membranes from spinach and for detergent-solubilized PSII core complexes from *Synechocystis* PCC 6803.[11] In the case of the core complexes, the Q_B site is the most exposed to the surrounding medium because the core complexes are solubilized and not embedded in native membrane sheets. In addition, core complexes lack associated light-harvesting complexes that could further shield the Q_B-binding site. The PSII membranes, however, occur as membrane fragments with significantly less exposure of the Q_B sites to the aqueous solution. And, the thylakoid membranes contain both PSI and PSII units within intact membranes that block access to the intermembrane proteins by charged hydrophilic groups. The O_2-evolution inhibition curves shown in Figure 4 and the corresponding pI_{50} values in Table 3 support the expected trend in the Q_B site accessibility by **4** because the pI_{50} values appear to depend on the degree of accessibility to the Q_B pocket. The core complexes show the largest pI_{50} value followed by the PSII membranes and finally by the thylakoid membranes. Because both **4** and **7** have a hydrophilic Fe^{III}−(EDTA) group, accessibility from the lipid surface would be restricted the most in thylakoid membranes, followed by PSII membranes and finally the PSII core complexes. These observations are in agreement with experiments by Gray and co-workers with charged pentammine ruthenium complexes.[28] They have reported that hydrophilic charged metal-complexes prevent penetration into the hydrophobic sites within the protein. On the other hand, DCMU and herbicides with BOC-protected amines are uncharged and possess hydrophobic groups that can interact favorably with the hydrophobic polypeptide residues of the binding pocket. These herbicides are observed to bind the Q_B site with little hindrance from the lipid network. Thus, the different pI_{50} values observed for the series of herbicide derivatives and sample types suggest that a combination of electrostatic, hydrophilicity and accessibility factors are at play in determining the strength of inhibition.

Table 3: pI_{50} Values for Inhibition of O_2-Evolution Activity from Different Sample Types Using **4** at 25 °C

sample type	pI_{50}
thylakoid membranes	~ 2
spinach PSII membranes	3.4
Synechocystis PCC 6803 core complexes	3.7

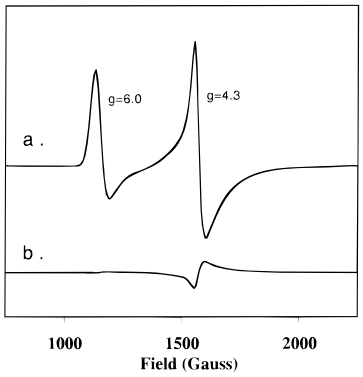

Figure 5. EPR signals from the Fe^{III}−(EDTA) moiety of **4** at $g = 4.3$ and from myoglobin at $g = 6.0$ added to a PSII membrane sample as an internal standard. a) Dark scan, (b) scaled difference between the spectrum after 8 min illumination at 225 K and the above dark scan. The negative amplitude of the difference signal compared to no change in the myoglobin signal is indicative of reduction of the Fe^{III}−(EDTA) moiety upon continuous illumination at 225 K.

Turnover Control in PSII at 225 K. Turnover control experiments were performed at 225 K in samples of PSII membranes containing 0.7 mM of **4**. On the basis of the pI_{50} value of 3.4 (Table 2), approximately a 12-fold excess of **4** was added to ensure that at least 50% of the Q_B-binding site was occupied and that the S_2 to S_3 conversion would produce a detectable change in the EPR signal of the Fe^{III}−(EDTA) acceptor. Although adding a higher concentration of **4** would lead to a higher occupancy of the Q_B-binding site, the change of the Fe^{III}−(EDTA) EPR signal would be more difficult to measure. Figure 5a shows the low-field EPR spectrum of a dark-adapted sample with the myoglobin and the Fe^{III}−(EDTA) signals at $g = 6.0$ and $g = 4.3$, respectively. Figure 5b shows the light-minus-dark difference EPR signals in the same sample after 8 min of illumination at 225 K. It can be observed that there is a loss of 9 ± 4% of the Fe^{III}−(EDTA) acceptor signal and no change in the myoglobin (internal standard) signal. The PSII sample concentration was 61 μM (based on the [Chl] and calculated using 200 Chl/PSII). Because the Q_B sites are expected to be 52% occupied by the herbicide (based on Figure

(25) Draber, W.; Tietjen, J.; Kluth, J. F.; Trebst, A. *Angew. Chem., Int. Ed. Engl.* **1990**, *30*, 1621−1633.
(26) Omokawa, H.; Takahashi, M. *Pest. Biochem. Physiol.* **1994**, *50*, 129−137. (b) Fedke, C. *Biochemistry and Physiology of Herbicide Action*; Springer-Verlag: New York, 1982.
(27) Asami, T.; Koike, H.; Inoue, Y.; Takahashi, N.; Yoshida, S. *Z. Naturforsch.* **1988**, *43*c, 857−861.
(28) (a) Gray, H. B. *Chem. Soc. Rev.* **1986**, *15*, 17. (b) Bowler, B. E.; Raphael, A. L.; Gray, H. B. *Prog. Inorg. Chem.* **1990**, *38*, 259−322.

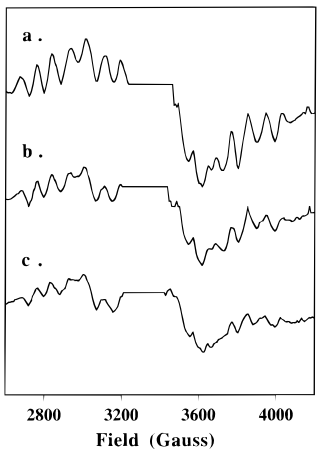

Figure 6. EPR spectra of the PSII membranes in the presence of 0.7 mM of **4** showing the S_2-multiline signal. (a) Spectrum after 3.5 min continuous illumination at 195 K, (b) spectrum after 2.0 min continuous illumination at 225 K, (c) spectrum after a total of 8 min illumination at 225 K. The narrow $Tyr_D^{\bullet}$ signal at 3300 G has been deleted for clarity.

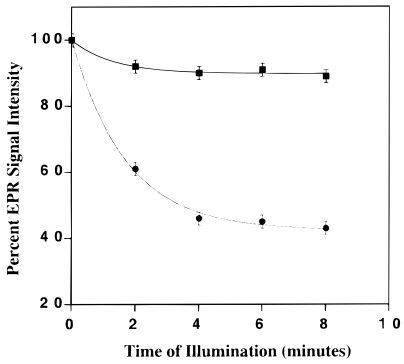

Figure 7. Percent EPR signal intensity changes upon continuous illumination of PSII membranes with 0.7 mM **4** at 225 K: S_2-multiline signal (●), Fe^{III}−(EDTA) of **4** (■). The amplitudes of the S_2-multiline and Fe^{III}−(EDTA) of **4** signals measured following the 195 K illumination were normalized to a value of 100% prior to proceeding to the 225 K illuminations. The lines represent exponential fits to the data for first-order decay kinetics at 225 K. The error bars represent 4% experimental uncertainty in the measurement of the data points.

3), we expect that the Fe^{III}−(EDTA) signal would decrease by approximately 4.6% based on the ratio of the concentrations of the Q_B site bound herbicide to the PSII sample. The slightly greater measured loss in the Fe^{III}−(EDTA) signal may be due to experimental uncertainty.

Figure 6 shows the corresponding decrease in the S_2-multiline EPR signal upon illumination at 225 K. For untreated samples with 195 K illumination, the dark adapted S_1 state can progress only to the S_2 state in almost 100% yield without undergoing further turnover.[29] However, illumination at 225 K allows advance to the S_3 state, provided that there is an electron acceptor species at the Q_B site. Figure 6a shows the S_2-multiline EPR signal acquired after a 3.5 min illumination at 195 K, Figure 6b shows the S_2-multiline signal upon continuous illumination at 225 K for 2 min and Figure 6c shows the S_2-multiline signal after a total of 8 min (a sequence of four 2 min illuminations). The intensity of the S_2-multiline signal was observed to decay during illumination at 225 K. Figure 7 shows the normalized plots representing the percent change of the S_2-multiline and Fe^{III}−(EDTA) acceptor EPR signals as a function

(29) dePaula J. C.; Innes, J. B.; Brudvig, G. W. *Biochemistry* **1985**, *24*, 28−34.

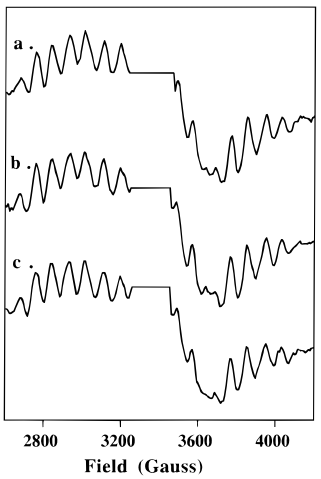

Figure 8. EPR spectra of the PSII membranes in the presence of 0.02 mM DCMU and 0.7 mM **4** showing the S_2-multiline EPR signal. (a) Spectrum after 3.5 min continuous illumination at 195 K, (b) spectrum after 2.0 min continuous illumination at 225 K, (c) spectrum after a total of 8 min illumination at 225 K. The narrow $Tyr_D^{\bullet}$ signal at 3300 G has been deleted for clarity.

of the illumination time. As expected, the Fe^{III}−(EDTA) acceptor and the S_2-multiline EPR signal intensities decrease due to turnover of the S_2 to the S_3 state with a concomitant Fe^{III} to Fe^{II} reduction of the acceptor. As shown in Figure 7, approximately half of an equivalent of Fe^{III}−(EDTA) was reduced during the first few minutes of illumination and prolonged illumination gave no further turnover. This is consistent with **4** accepting one electron while bound to the Q_B site, and with no exchange of **4** into and out of the Q_B site during the period of illumination at 225 K. The 60% loss of the S_2-multiline signal mirrors the percent O_2-evolution inhibition by **4** at 700 μM concentration, because the inhibition curve of **4** (Figure 3) shows that only 52% of the centers are inhibited at 0.7 mM concentration of **4**.

To verify that the S_2 to S_3 turnover occurs via electron transfer to **4** bound to the Q_B site, control experiments were performed with samples treated with 200 μM DCMU prior to treatment with or without 700 μM of **4** in the same PSII sample. Because DCMU has a greater affinity for the Q_B-binding site (pI_{50} = 6.5, Table 2), it would preferentially occupy the Q_B-binding site in PSII, while **4** would be randomly dispersed on the surrounding surface sites or remain in solution. Figures 8 and 9 show the EPR spectra and the corresponding intensities of the Fe^{III}(EDTA) and S_2-multiline signals as a function of the illumination time at 225 K. It is apparent from Figures 8 and 9 that there is no significant decay of the S_2 multiline and Fe^{III}−(EDTA) EPR signals even after 8 min of continuous illumination. The observed residual decrement of 15 ± 4% in the S_2-multiline signal may be due to incomplete occupancy of the Q_B sites, to transfer of electrons to dioxygen[18] dissolved in the sample or to inherent experimental errors contributing to the EPR measurement. The fact that the S_2-multiline and the Fe^{III}−(EDTA) signal intensities remain constant with 225 K illumination further indicates that there are no surface pathways of electron transfer to the Fe^{III}−(EDTA) acceptor of **4**. This control experiment supports the conclusion that **4** accepts an electron while bound in the Q_B site and allows for S_2 to S_3 state turnover.

Similar turnover experiments in PSII membranes were also performed at 225 K using 500 μM of **7** which has an Fe^{III}−(EDTA) acceptor with a pentane spacer linked to the dimethyl phenylurea moiety. It was observed that 65% of the S_2-multiline signal decayed away after 8 min of continuous illumination at

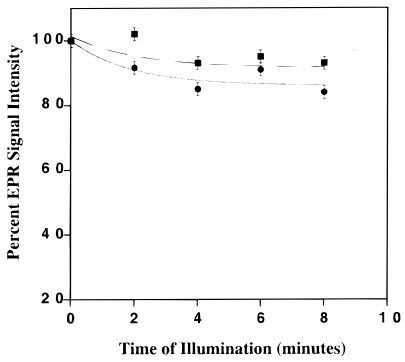

Figure 9. Percent changes of the S_2-multiline (●) and Fe^{III}−(EDTA) of **4** (■) EPR signals in the presence of 0.020 mM DCMU and 0.7 mM of **4**. The amplitudes of the S_2-multiline and Fe^{III}−(EDTA) of **4** signals measured following the 195 K illumination were normalized to a value of 100% prior to proceeding to the 225 K illuminations. The lines represent exponential fits of the data points and the error bars reflect 4% uncertainty level in the measurements.

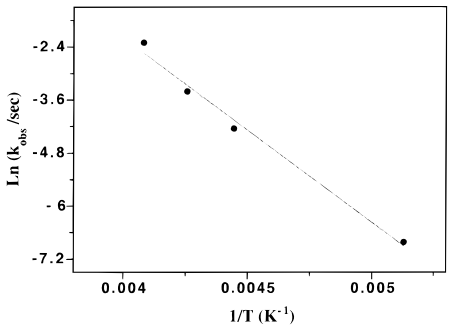

Figure 10. Arrhenius plot of the natural logarithm of the rate constant (k_{obs}) versus the inverse temperature. The line is the linear least-squares fit to the data.

225 K. A slightly higher loss of the S_2-multiline signal than observed with **4** suggests that a slightly greater percentage of the Q_B sites are occupied by **7,** in agreement with the respective pI_{50} values. As in the case of **4**, a 9 ± 4% loss in the Fe^{III}−(EDTA) EPR signal was observed with a concomitant loss in the S_2-multiline signals in the 225 K illumination experiment indicating that approximately one equivalent of the Fe^{III}−(EDTA) acceptor underwent reduction upon continuous illumination.

Further S_2 to S_3 state turnover experiments were performed with samples containing **4** at various temperatures ranging from 195 to 245 K to investigate the temperature dependence of the rate of electron transfer (k_{obs}) to the Fe^{III}−(EDTA) acceptor of **4**. As in the case of the 225 K illumination experiments, the S_2-multiline EPR signal intensity was observed to decrease by 60% upon continuous illuminations with a concomitant 9 ± 4% loss in intensity of the Fe^{III}−(EDTA) acceptor of **4** at 235 and 245 K illumination temperatures. In the case of 195 K illumination, the S_2-multiline signal decayed away by about 40% of the initial value upon continuous stepwise illumination up to 23 min. The observed S_2-multiline EPR signal decay lifetimes, ($\tau = 1/e$), varied with the temperature of illumination and the observed decays were fit using an exponential function assuming first-order decay kinetics as shown in Figure 7. An Arrhenius plot of the observed rate constant, k_{obs}, (sum of the various rates including both donor and acceptor side effects) as a function of the illumination temperature for **4** is shown in Figure 10, and gives an effective activation barrier, E_A, of 35 ± 5 kJ mol^{-1}. It was also observed that both **4** and **7** show comparable S_2-multiline decay lifetimes at 225 K suggesting that the rate of electron transfer to the Fe^{III}−(EDTA) acceptor may not depend on the hydrocarbon spacer length at least up to 5 carbon atom spacer length.

Discussion

Previous EPR studies with the redox-active herbicide PNPDU have shown that a controlled two-electron turnover from the S_1 to S_3 state can occur successfully by continuous illumination at 250 K, forming the S_3 state with a 75% yield.[8] However, two-electron turnover of PSII at lower temperatures could not be achieved with PNPDU because of the protonation requirement for electron transfer to the nitroxyl group (Scheme 2). The current results show that the two-step turnover from S_1 to S_3 turnover can be successfully achieved with **4** and **7** at much lower temperatures than previously possible with PNPDU, mainly because the Fe^{III}−(EDTA) electron acceptor of the herbicides does not require protonation for electron transfer. Furthermore, because both **4** and PNPDU have only moderate binding affinity for the Q_B binding site, the low-temperature (<250 K) studies with **4** effectively minimize the problem of multiple turnovers due to herbicide dissociation. The yield of the S_3 state was about 60−65% in the majority of the experiments with spinach PSII. This yield correlates well with the extent of O_2-evolution inhibition in spinach PSII membranes by the redox-active herbicides; because of the reduced affinity for the Q_B site of **4** and **7** relative to PNPDU, only ∼50−60% of the Q_B sites were occupied at the concentrations used in our studies. Although the present study uses spinach PSII with moderate (700 μM) concentrations of **4** and **7** to demonstrate the S_2 to S_3 conversion of the OEC, a greater than 90% yield of the S_3 state could be achieved by using *Synechocystis* PCC 6803 core complexes and a higher concentration of **4**. In comparison to PNPDU, which exhibits a large EPR signal at $g \approx 2$ that obscures the EPR signal from PSII species, the nonoverlapping EPR signal of the Fe^{III}−(EDTA) moiety at $g = 4.3$ permits the observation of both the herbicide and the OEC signals while monitoring the S_2 to S_3 conversion.

The O_2-evolution studies with metal-containing redox-active herbicides **4** and **7** suggest that the dimethylphenylurea group enables the Fe^{III}−(EDTA) acceptor to dock in the Q_B-binding pocket because Fe^{III}−(EDTA) by itself does not inhibit O_2-evolution activity or accept electrons from PSII at low temperatures. However, the Q_B site affinity of **4** and **7** are compromised due to the presence of the hydrophilic Fe^{III}−(EDTA) group. The structural details of the Q_B-binding pocket in plant PSII would benefit the design of tighter binding redox-active herbicides. The currently available 8 Å resolution structure of plant PSII, however, is still insufficient to provide a detailed structure of the plant Q_B site.[30] Nonetheless, the high-resolution crystal structures of the analogous bacterial reaction center (bRC) from *Rb. sphaeroides* and *Rb. viridis* have provided structural insight into the Q_B-binding pocket.[31] The crystal structure of the bRC Q_B site shows a hydrophobic pocket with internal dimensions of ∼10 Å × ∼8 Å. Crystal structures with the herbicides terbutryn and atrazine bound inside the Q_B-binding pocket reveal specific hydrogen bonding interactions of the triazine nitrogens with Ser L223, Ile L224, His L190, Phe L216, Glu L212, and Tyr L222 in conferring the tight binding affinity.[32] Although crystal structures with DCMU

(30) Rhee, K.-H.; Morris, E. P.; Barber, J.; Kühlbrandt, W. *Nature* **1998**, *396*, 283−286.
(31) Deisenhofer, J.; Michel, H. *Science* **1989**, *245*, 1463−1473.
(32) Lancaster, C.; Roy, D.; Michel, H. *Photosyn. Res.* **1996**, *48*, 65−74. (b) Lancaster, C.; Roy, D.; Michel, H. *J. Mol. Biol.* **1999**, *286*, 883−898.

bound in the Q_B pocket are not presently available, we can infer that the urea group forms hydrogen bonds to the polypeptide residues similar to triazines and quinones. The dimethylphenylurea group of **4** and **7** can be envisioned to be docked at the Q_B site and the Fe^{III}−(EDTA) acceptor to project out of the Q_B-binding pocket. Furthermore, by analogy to the bRC structure, where the quinone tail points toward the $Pheo_A$ molecule, it is possible that the Fe^{III}−(EDTA) moiety is oriented toward the $Pheo_A$. This would account for the evidence that the Fe^{III}−(EDTA) moiety is reduced by $Pheo_A^-$ rather than Q_A^- (see below).

To address the pathway of electron transfer to the Fe^{III}−(EDTA) moiety, a dark-incubation experiment of PSII membranes with 700 μM of **4** at 225 K was performed following the 3.5 min illumination at 195 K. Dark-incubation of the illuminated sample for 15 min at 225 K did not produce a significant loss in the Q_A^-, the S_2-multiline or the Fe^{III}−(EDTA) acceptor EPR signals of the herbicide from that of the 195 K illumination experiment. Electron transfer to the Fe^{III}−(EDTA) acceptor via Q_A^- (Scheme 3) would result in a decrease of the Q_A^- EPR signal during dark incubation. However, the Q_A^- EPR signal remains constant indicating that Q_A^- does not donate an electron to the Fe^{III}−(EDTA) acceptor group in the dark at 225 K. Continuous 2 min illumination at 225 K following the 15 min dark-incubation, however, produced a 50% loss in the S_2-multiline EPR signal and a 10 ± 4% loss in the Fe^{III}−(EDTA) signal indicating reduction of approximately one equivalent of **4**. Although the assumed conventional electron-transfer pathway to the Q_B site via Q_A^- cannot be ruled out, the current results suggest that pheophytin ($Pheo_A^-$) may participate in the electron-transfer process as it is located in close proximity, ∼15 Å, to the Q_B-binding site and has a lower reduction potential (−0.5 V vs NHE) than Q_A (−0.1 V vs NHE). Regardless of whether electron transfer occurs via $Pheo_A^-$ or via Q_A^-, electron transfer would still involve a long-range interaction because Q_A^- is separated from Q_B by ∼ 15 Å based on homology with the bRC.[31] In addition, the Fe^{III}−(EDTA) moiety of **4** is further separated by ∼13 Å from the phenylurea moiety which is expected to bind in the Q_B pocket. Thus, electron transfer to the Fe^{III}−(EDTA) acceptor would involve long-range through space and sigma-bond coupling pathways. The hydrocarbon chain linkers in these redox-active herbicides may provide an efficient coupling pathway as in the cytochrome P450 electron-transfer studies by Wilker et al.[10]

It was observed that the rate of two-electron turnover depended upon the temperature of illumination. An Arrhenius analysis yielded an activation energy of 35 ± 5 kJ/mol. In previous studies with the bRC, a large activation barrier of 56 kJ/mol was found for Q_A^- to Q_B electron transfer.[33] The large activation barrier was thought to be due to a large reorganization energy or a conformational gating for electron transfer.[34] The conformational gating process is associated with protein dynamics that allow the quinone to move into the proximal position from the distal position enabling electron transfer from Q_A^- to Q_B. Because the bRC and PSII are structurally homologous with similar electron-acceptor sides, the electron-transfer mechanism from Q_A^- to Q_B in PSII could likely involve similar herbicide and protein structural rearrangements in the Q_B-binding pocket during the electron-transfer event.

The current results show that there are several advantages of using metal-containing redox-active herbicides in studying intermediate states of the PSII photocycle. First and most importantly, these redox-active herbicides enable the high-yield preparation of the S_3 state for future spectroscopic studies of the S_3 state. Although low-temperature turnover studies of spinach PSII membranes show that the S_3 state can be formed in 60−65% yield, inhibition studies suggest that yields as high as ∼90% could be obtained when using high concentrations of **4** with PSII core complexes, because **4** binds much better to the PSII core complexes owing to the greater accessibility of the Q_B site to the aqueous phase. Second, these metal-containing herbicides allow for the possibility of tuning the energetics to investigate the long-range coupling and electron-transfer mechanisms in PSII by allowing variation in the coordinating ligands. For example, [M^{III}-(EDTA)L] acceptors (where M = Ru) has an open sixth coordination site that could be coordinated by various ligands (L) to tune the driving force ($\Delta G°$) of electron transfer.[35] The dependence of the rate (k_{obs}) on the driving force ($\Delta G°$) would provide further insight into the mechanism of electron transfer in PSII.

Besides enabling electron-transfer studies and the high-yield preparation of the S_3 state, these metal-containing herbicides could afford the possibility for studying previously inaccessible intermediate states in photosystem II. For example, if the redox-active herbicide accepts electrons at 195 K faster than the S_2 to $Y_z^\bullet$ electron-transfer rate, then continuous illumination could lead to the generation of the $S_2Y_z^\bullet$ state in an uninhibited PSII sample.[9] This intermediate state is typically prepared when inhibited PSII samples are continuously illuminated at 273 K and rapidly frozen to 77 K. However, one drawback is that the inhibitory treatments (Ca^{2+} depletion, Cl^- depletion or addition of acetate) could lead to structural perturbation of the OEC. Thus, it would be of great interest to generate and study this state without perturbing the OEC. Furthermore, using a redox-active herbicide that can accept multiple electrons, for example by coupling biferrocence[36] (two iron atoms) to an atrazine or DCMU binding functionality, could lead to trapping and study of the elusive S_4 state.

Acknowledgment. This work was supported by the National Institutes of Health Grant GM 32715. We thank the research group of Professor Schepartz at Yale University for use of their HPLC instrument. We thank Susan deGala for obtaining the X-ray crystal structure and Michael Reifler for helpful discussions about synthesis and for preparing the His-tagged PSII core complexes. We also thank Olaf Kievit for his assistance with electrochemical measurements.

Supporting Information Available: Tables of crystallographic data including atomic coordinates, bond angles and bond lengths, and anisotropic displacement parameters (PDF). An X-ray crystallographic file, in CIF format. This material is available free of charge via the Internet at http://pubs.acs.org.

JA994138X

(33) (a) Macino, L. J.; Dean, D. P.; Blankenship, R. E. *Biochim. Biophys. Acta* **1984**, *764*, 46−54. (b) Kleinfeld, D.; Okamura, M. Y.; Feher, G. *Biochim. Biophys. Acta* **1984**, *766*, 126−140. (c) Li, J. L.; Gilroy, D.; Tiede, D. M.; Gunner, M. R. *Biochemistry* **1998**, *37*, 2818−2829.

(34) According to studies performed on the bacterial reaction center (bRC), conformational gating is thought to limit the rate of electron transfer from Q_A^- to Q_B. For example, see: (a) Graige, M. S.; Okamura, M. Y. *Proc. Natl. Acad. Sci. U.S.A.* **1998**, *95*, 11679−11684. In addition, the second electron-transfer step from Q_A^- to Q_B^- is limited by the rate of proton transfer to Q_B^-. See: (b) Graige, M. S.; Paddock, M. L.; Bruce, J. M.; Feher, G.; Okamura, M. Y. *J. Am. Chem. Soc.* **1996**, *118*, 9005−9016. (c) Graige, M. S.; Paddock, M. L.; Bruce, J. M.; Feher, G.; Okamura, M. Y. *Biochemistry* **1999**, *38*, 11465−11473.

(35) (a) Masubara, T.; Creutz, C. *Inorg. Chem.* **1979**, *18*, 1956−1966. (b) Diamantis, A. A.; Dubrawski, J. V. *Inorg. Chem.* **1983**, *22*, 1934−1946.

(36) (a) Morrison, W. H.; Hendrickson, D. N. *Inorg. Chem.* **1975**, *14*, 2331−2346. (b) Creutz, C. *Prog. Inorg. Chem.* **1983**, *30*, 1−73.